

Jamming in Systems With Quenched Disorder

C.J. Olson Reichhardt¹, E. Groopman^{1,2}, Z. Nussinov², and C. Reichhardt¹

¹*Theoretical Division, Los Alamos National Laboratory, Los Alamos, New Mexico 87545, USA*

²*Department of Physics, Washington University, St. Louis, Missouri 63160, USA*

(Dated: August 10, 2018)

We numerically study the effect of adding quenched disorder in the form of randomly placed pinning sites on jamming transitions in systems that jam at a well defined point J in the clean limit. Quenched disorder decreases the jamming density and introduces a depinning threshold. The onset of a finite threshold coincides with point J at the lowest pinning densities, but for higher pinning densities there is always a finite threshold even well below jamming. We find that proximity to point J strongly affects the transport curves and noise fluctuations, and observe a change from plastic behavior below jamming, where the system is highly heterogeneous, to elastic depinning above jamming. Many of the general features we find are related to other systems containing quenched disorder, including the peak effect observed in vortex systems.

PACS numbers: 64.60.Ht, 83.60.Bc, 83.80.Fg, 74.25.Wx

When a collection of particles such as grains is at low densities with little grain-grain contact, the system acts like a liquid in response to an external drive. At higher densities, however, significant grain-grain contacts occur and the system responds like a rigid solid, exhibiting a jamming transition where the grains can become stuck under an external drive [1, 2]. The jamming density is termed point J in simple systems such as bidisperse disk assemblies [1–4]. An already jammed system can be unjammed by the application of shear [5–7] and numerous studies have focused on understanding jamming for varied grain shapes [8], interactions [9], temperatures [10], and external drives [11, 12]. Depinning is another example of a transition from a stuck or pinned state to a flowing state under an applied drive, and occurs for collectively interacting particles in quenched disorder such as vortices in type-II superconductors [13–15], colloids interacting with random or periodic substrates [16–18], and charge-density waves [19]. Above depinning, the particles pass from a stationary solid state into either a flowing solid or a fluctuating, liquidlike state [13, 15, 16]. Understanding how quenched disorder affects jamming and how jamming-unjamming transitions are related to depinning would have a great impact in both fields.

The first proposed jamming phase diagram for loose particle assemblies had three axes: inverse density, load, and temperature [1]. Here we propose that quenched disorder can form a fourth axis of the jamming phase diagram, and show that if a system has a well defined jamming transition in the absence of quenched disorder, proximity to point J is relevant even for strong quenched disorder. We also show that jammed or pinned states below point J show profoundly different behaviors in response to an external drive compared to states above point J . We find that for varied amounts of disorder, this system exhibits many features found in vortex matter [13, 20, 21] including a peak effect near point J , suggesting that jamming may be a useful way to understand

many of the phenomena found in systems with pinning. We study a two-dimensional (2D) bidisperse disk system with equal numbers of disks of each size that is known to exhibit jamming at a well defined density for zero temperature and load. The density is defined as the fraction ϕ of the system area that is covered by the disks. For a disk radius ratio of 1 : 1.4, in 2D the onset of jamming occurs at $\phi_J \approx 0.844$ [3, 5, 11, 22]. Since point J in this system is well defined in the absence of quenched disorder, we can determine how jamming changes when we add a small amount of quenched disorder in the form of randomly placed pinning sites. We also focus on distinguishing the effect of jamming from that of depinning. This is particularly important since even non-interacting particles that do not exhibit a jamming transition in the absence of quenched disorder can still exhibit a finite depinning threshold in the presence of disorder.

Simulation– We consider a 2D system of size $L \times L$ with periodic boundary conditions in the x and y -directions containing N disks that interact via a short range repulsive spring force. The sample is a 50:50 mixture of disks with interaction ranges r_A and r_B , where $r_A = 1.4r_B$. N_J is the number of particles in the sample at the jamming transition. To initialize the system, we place disks in nonoverlapping positions and then shrink all disks, add a few additional disks, and reexpand all disks while thermally agitating the disks until reaching the desired density. We employ overdamped dynamics where the equation of motion for the disks is $\eta d\mathbf{R}_i/dt = \sum_{i \neq j} k(R_{\text{eff}}^{ij} - |\mathbf{r}_{ij}|)(\mathbf{r}_{ij}/|\mathbf{r}_{ij}|)\Theta(R_{\text{eff}}^{ij} - |\mathbf{r}_{ij}|) + \mathbf{F}_p^i + \mathbf{F}_D$. Here the damping constant $\eta = 1$, $k = 200$, and $R_{\text{eff}}^{ij} = r_i + r_j$, where $r_{i(j)}$ is the radius of disk $i(j)$. The driving force $\mathbf{F}_D = F_D \hat{\mathbf{x}}$ is applied to all the disks uniformly. The pinning force \mathbf{F}_p^i is modeled as arising from N_p non-overlapping attractive parabolic traps with a maximum force of F_p and a cut-off radius of $r_A/2$ to ensure that only one grain can be trapped by any one pinning site. In the absence of other grains, an isolated grain will depin when $F_D > F_p$. In

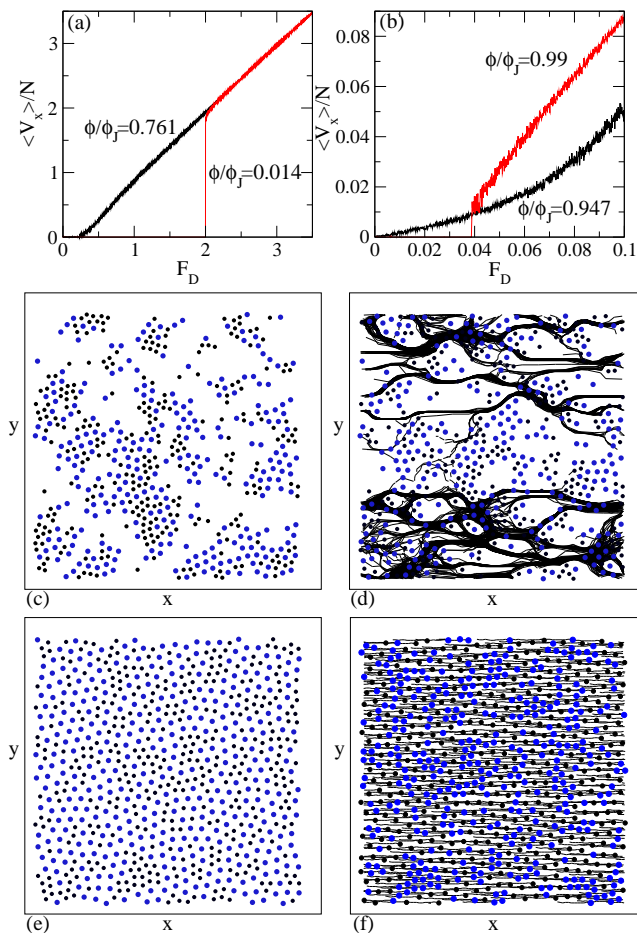


FIG. 1: (Color online) (a,b) The normalized average grain velocity $\langle V_x \rangle / N$ vs external drive F_D in samples with $F_p = 2.0$. (a) $N_p/N_J = 0.415$. Right (red) curve: at $\phi/\phi_J = 0.014$ depinning occurs at $F_c = 2.0$. Left (black) curve: at $\phi/\phi_J = 0.761$, F_c is much lower. (b) $N_p/N_J = 0.09267$. Lower (black) curve: at $\phi/\phi_J = 0.947$, there is no finite depinning threshold. Upper (red) curve: at $\phi/\phi_J = 0.99$, F_c is finite. (c) Disk positions in the pinned state for the system in (a) with $\phi/\phi_J = 0.761$. (d) The disk trajectories over a period of time for the system in (c) at $F_D = 0.25$ showing plastic flow above the depinning threshold. (e) Disk positions in the pinned state for the system in (c) with $\phi/\phi_J = 1.03878$. (f) The disk trajectories over a period of time for the system in (e) at $F_D = 1.1F_c$ showing elastic flow.

the absence of pinning, this model has been well studied and has a jamming density of $\phi_J \approx 0.844$ [3, 11]. To determine if the system is pinned, we measure the total average grain velocity $\langle V_x \rangle = \sum_{i=1}^N \mathbf{v}_i \cdot \hat{\mathbf{x}}$ as a function of F_D , where \mathbf{v}_i is the velocity of grain i . For most of the results presented, F_D is slowly increased in increments of $\delta F_D = 5 \times 10^{-6}$ and we wait 5×10^4 simulation time steps after each force increment to ensure that the system reaches a steady state response.

In Fig. 1(a,b) we plot $\langle V_x \rangle / N$ versus F_D for different pinning densities and particle densities, measured in

terms of N_p and ϕ_J . At $N_p/N_J = 0.415$ and $\phi/\phi_J = 0.014$ in Fig. 1(a), the system is pinned for drives up to $F_D = 2.0$. At this low density, there are no interactions between the disks and the depinning threshold F_c is solely determined by the pinning force. For the same pinning density at $\phi/\phi_J = 0.761$, there are more disks than pinning sites; however, as shown in Fig. 1(a), there is still a finite depinning threshold of $F_c = 0.27$. Since not all of the disks can be captured by pinning sites, the existence of a finite depinning threshold indicates that the disks trapped by pins must be blocking the flow of the disks that are not in pins. Thus, in pinned states such as that illustrated in Fig. 1(c), some form of jamming must be occurring. The depinning threshold can vanish when the pinning density is reduced, as shown in Fig. 1(b) for a sample with $N_p/N_J = 0.09267$ and $\phi/\phi_J = 0.947$. Here $F_c = 0$ and the velocity response is nonlinear. The depinning threshold remains zero as ϕ/ϕ_J is reduced until N drops below N_p and all the disks can be trapped, giving $F_c = F_p$. At high disk densities such as $\phi/\phi_J = 0.99$ in Fig. 1(b), F_c is finite. Figure 1(b) also shows an interesting crossing of the velocity-force curves, caused by the sudden jump in $\langle V_x \rangle / N$ at depinning for the $\phi/\phi_J = 0.99$ sample. The depinning is elastic for $\phi/\phi_J = 0.99$, so all the disks begin to move simultaneously at the same velocity with only small localized rearrangements of the disk packing. In contrast, for $\phi/\phi_J = 0.947$ the depinning is plastic. Some disks remain pinned while other disks move past, and the pinned disks do not depin until a much higher F_D is applied (not shown). An example of the plastic flow occurring at depinning appears in Fig. 1(d) for a sample with $N_p/N_J = 0.415$ and $\phi/\phi_J = 0.761$ at $F_D = 0.25$, above the depinning threshold. Certain disks are always pinned while rivers of disks flow around them. In the jammed state, the disk packing acts like a solid and a small number of pinning sites can trap all the disks, as in the sample with $N_p/N_J = 0.09267$ and $\phi/\phi_J = 0.99$ in Fig. 1(b). The depinning from the jammed state is elastic, as illustrated for $\phi/\phi_J = 1.03878$ in Fig. 1(e,f). Below jamming in samples containing a small number of pinning sites, such as the $N_p/N_J = 0.09267$ and $\phi/\phi_J = 0.947$ sample shown in Fig. 1(b), some but not all of the disks can be immobilized, so the depinning is plastic.

Figure 2(a) shows F_c versus ϕ/ϕ_J for a series of different values of N_p/N_J , and Fig. 2(b) shows a blowup of the same data near $\phi/\phi_J = 1.0$. For $N_p/N_J > 0.138$ the depinning threshold is finite for all ϕ/ϕ_J . For $N_p/N_J \leq 0.138$ at low ϕ/ϕ_J , the depinning force reaches its maximum possible value of $F_c = F_p = 2.0$ since all the disks can be trapped by pinning sites without any overlap. There is a region of intermediate ϕ/ϕ_J where there is no depinning threshold. At higher ϕ/ϕ_J , F_c becomes finite again and the system undergoes plastic depinning. The value of F_c increases with increasing ϕ/ϕ_J in this regime until F_c peaks near $\phi/\phi_J = 1.0$ when the system

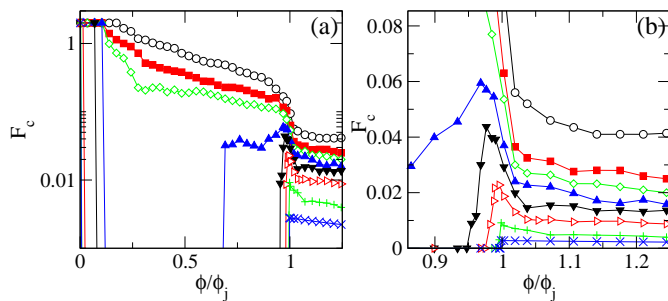


FIG. 2: (Color online) F_c vs ϕ/ϕ_J for $N_p/N_J = 0.828$ (\circ), 0.415 (red \blacksquare), 0.277 (green \diamond), 0.138 (blue \blacktriangle), 0.09267 (\blacktriangledown), 0.0346 (red \triangleright), 0.00692 (green $+$), and 0.00138 (blue \times). (a) A log-linear plot over the full range of ϕ/ϕ_J shows that the depinning threshold is always finite for $N_p/N_J > 0.138$, while for $N_p/N_J \leq 0.138$ there is a pinned regime at low ϕ/ϕ_J when all the disks are trapped by pinning sites and another regime of finite F_c at high ϕ/ϕ_J where jamming occurs. (b) A blowup of the region near $\phi/\phi_J = 1.0$ shows that the onset of jamming is marked by either a drop in F_c for the higher pinning densities or a peak in F_c for the lower pinning densities.

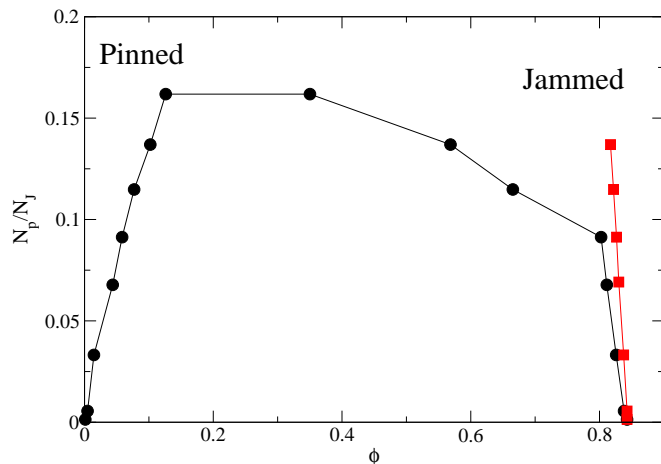


FIG. 3: (Color online) Black circles: The value of N_p/N_J at which a finite depinning force first appears vs ϕ . Red squares: The value of N_p/N_J at which F_c reaches its peak value vs ϕ . The system depins elastically for ϕ just above the peak value of F_c . For small ϕ , all of the particles are directly pinned at pinning sites, while for ϕ close to $\phi_J = 0.844$, the particles are pinned due to jamming.

jams. At jamming, in principle a single pinning site could pin the entire granular packing; however, we find that F_c at jamming decreases as the pinning density is reduced. At and above jamming, the depinning becomes elastic and F_c drops with increasing ϕ/ϕ_J due to the increasing stiffness of the jammed solid.

Using velocity force curves, we identify the onset of a finite depinning threshold as a function of ϕ for different values of N_p/N_J , as well as the value of ϕ at which F_c reaches its peak value for ϕ near ϕ_J . The result is shown in Fig. 3. There is a dome feature connecting the low

ϕ limit, where the disks are directly pinned at pinning sites, with the high ϕ limit, where the pinning occurs when the grains become jammed. Near ϕ_J we find that the quenched disorder density N_p/N_J can be considered as a new axis of the jamming phase diagram, and that the jamming density decreases with increasing pinning density. Although the onset of jamming can be defined as coinciding with the appearance of a finite depinning threshold, it could also be defined as coinciding with the transition from plastic to elastic depinning, where F_c reaches its peak value. Figure 3 shows that these two definitions are not identical but track each other closely in the region near ϕ_J . The onset of elastic depinning continues to produce a peak in F_c up to the highest pinning densities we have considered.

We can make a simple argument for how quenched disorder reduces the jamming density. The average distance between pinning sites is $l_p \propto \rho_p^{-1/2}$, where $\rho_p = N_p/L^2$. We can estimate a correlation length ξ by assuming that ξ grows as jamming is approached according to $\xi \propto (\phi_J - \phi)^{-\nu}$. Jamming should occur when $l_p = \xi$, or when $\rho_p \propto (\phi_J - \phi)^{2\nu}$. A fit of the onset of finite F_c for $\phi > 0.8$ or a fit to the peak value of F_c both give a linear dependence on ϕ , implying that $\nu = 0.5$. This value is close to some threshold predictions [23]; however, caution must be taken in comparing our exponent to systems without quenched disorder, since the presence of quenched disorder or the fact that we are driving our system could fundamentally change the nature of the jamming compared to the disorder free case, and additional corrections to scaling could be relevant [24].

The onset of jamming can also be detected by analyzing the velocity noise fluctuations using the power spectrum $S(f)$ obtained from the time series of the average disk velocities, $S(f) = |\int \exp(-i2\pi ft) \langle V_x \rangle(t) dt|^2$. The noise power S_0 is defined to be the integrated noise power in the lowest octave of the spectrum. We take $F_D = 1.1F_c$. Figure 4(a) shows S_0 versus ϕ for $N_p/N_J = 0.277$ and Fig. 4(b) shows the same quantity for $N_p/N_J = 0.0346$. For $N_p/N_J = 0.277$, the noise power S_0 is low for $\phi/\phi_J < 0.3$ since there are very few collective interactions at these low densities that could give rise to low frequency noise. S_0 decreases rapidly with increasing ϕ/ϕ_J for $\phi/\phi_J > 0.95$ after the system jams and transitions to elastic depinning. At intermediate ϕ/ϕ_J , large velocity fluctuations occur and produce a broad band noise signal, as shown in Fig. 4(c) for $\phi/\phi_J = 0.968$ where the depinning is plastic. The solid line in Fig. 4(c) is a fit to $1/f^{0.9}$. The appearance of $1/f$ type noise is known to be associated with plastic depinning [15, 20]. For $\phi/\phi_J = 1.141$ in the elastic depinning regime, Fig. 4(c) shows that the noise power is considerably reduced and the spectrum has a peak at finite frequencies with several higher harmonics, indicative of a narrow band noise signal. The appearance of narrow band noise in driven systems with quenched disorder is

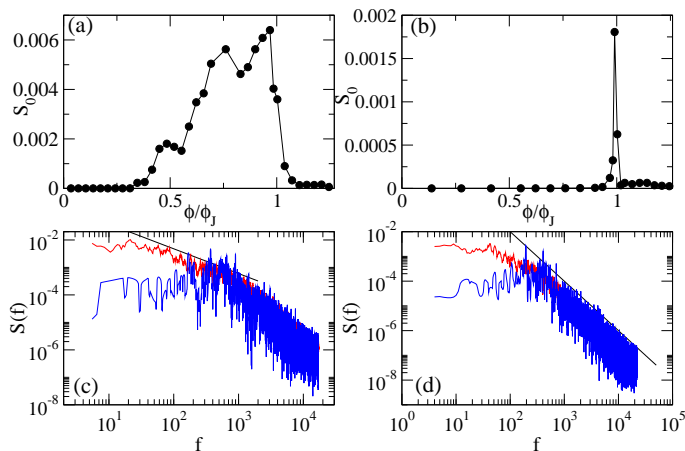


FIG. 4: (Color online) (a,b) The noise power S_0 obtained from the time series of the velocity fluctuations vs ϕ/ϕ_J for $F_D = 1.1F_c$. (a) $N_p/N_J = 0.277$. S_0 drops at the onset of jamming and at low ϕ/ϕ_J . (b) $N_p/N_J = 0.0346$. There is a pronounced peak in S_0 just below jamming. (c) The power spectrum $S(f)$ vs f from the system in (a) for (upper red curve) $\phi/\phi_J = 0.968$ where the depinning is plastic and (lower blue curve) $\phi/\phi_J = 1.141$ where the depinning is elastic and a narrow band noise signal appears. The solid black line is a fit to $1/f^{0.9}$. (d) $S(f)$ vs f for the system in (b) for (upper red curve) $\phi/\phi_J = 0.989$ and (lower blue curve) $\phi/\phi_J = 1.141$ showing narrow band noise in the jammed phase. The solid black line is a fit to $1/f^2$.

associated with the formation of a moving solid [19, 25] and is commonly referred to as a washboard frequency. This is consistent with the moving jammed packing acting like a rigid solid. For the smaller pinning density of $N_p/N_J = 0.0346$, Fig. 4(b) shows a pronounced peak in S_0 at $\phi/\phi_J = 0.989$, which corresponds to a density just below the peak in F_c . S_0 then drops off rapidly as the system enters the jammed phase and depins elastically. In Fig. 4(d) we plot the power spectra for $\phi/\phi_J = 0.989$ and $\phi/\phi_J = 1.141$ for $N_p/N_J = 0.0346$. There is broad band noise in the plastic flow regime at $\phi/\phi_J = 0.989$ and narrow band noise in the elastic flow regime at $\phi/\phi_J = 1.141$.

The depinning-jamming transition we observe has many similarities to the peak effect phenomenon in type-II superconductors with vortices moving through random disorder. The peak effect can occur as a function of vortex density. At low densities, the depinning threshold is high since vortices can be pinned individually. At intermediate densities, the depinning threshold remains at a low value until some higher density is reached where there is a significant increase in the depinning threshold to a peak value. This is associated with a large increase in the noise power [13, 20, 21]. The peak effect and the noise features become more prominent for cleaner samples with less pinning [21]. All these features are captured in our results. The standard interpretation of the peak effect is that it marks a transition from a weakly pinned solid to a

more strongly pinned disordered state. Our results suggest that the peak effect may be a general phenomenon in other systems with quenched disorder close to some type of phase transition.

In summary, we show how jamming behavior changes with the addition of quenched disorder using a simple model of bidisperse disks that exhibit a well defined jamming density ϕ_J in the absence of quenched disorder. We propose that quenched disorder represents a new axis of the jamming phase diagram and that increasing quenched disorder density decreases the disk density at which the system jams. At low disorder densities, the disk density at which a finite depinning threshold appears coincides with point J. There is also a reentrant finite depinning threshold at low disk densities when all the disks are directly pinned. We find a maximum in the depinning threshold just at the onset of jamming for low disorder densities. When the disorder density is sufficiently large, the depinning threshold is finite for all disk density values; however, proximity to ϕ_J produces clear effects in the form of features in the velocity force curves as well as noise fluctuation signatures. Below jamming, the depinning is characterized by plastic flow and $1/f$ noise characteristics with strong heterogeneities in the system, while above jamming, the depinning is elastic with all the particles moving together and is characterized by a washboard noise. For high disorder density the onset of jamming is associated with a drop in the depinning threshold as opposed to the peak in depinning found at low disorder density. Our results show many similarities to the peak effect observed in high-temperature superconductors where a peak in the depinning threshold occurs at both low and high vortex densities. Our results should be relevant for systems exhibiting depinning transitions and jamming.

This work was carried out under the auspices of the NNSA of the U.S. DoE at LANL under Contract No. DE-AC52-06NA25396. Z.N. was supported by NSF DMR-1106293 at WU.

-
- [1] A.J. Liu and S.R. Nagel, *Nature (London)* **396**, 21 (1998).
 - [2] A.J. Liu and S.R. Nagel, *Annu. Rev. Condens. Matter Phys.* **1**, 347 (2010).
 - [3] C. S. O'Hern, L.E. Silbert, A.J. Liu, and S.R. Nagel, *Phys. Rev. E* **68**, 011306 (2003).
 - [4] C. Zhao, K. Tian, and N. Xu, *Phys. Rev. Lett.* **106**, 125503 (2011).
 - [5] P. Olsson and S. Teitel, *Phys. Rev. Lett.* **99**, 178001 (2007); M. Otsuki and H. Hayakawa, *Phys. Rev. E* **83**, 051301 (2011); P. Olsson and S. Teitel, *Phys. Rev. E* **83**, 030302(R) (2011).
 - [6] D. Bi, J. Zhang, B. Chakraborty, and R.P. Behringer, *Nature (London)* **480**, 355 (2011).
 - [7] C. Heussinger and J.-L. Barrat, *Phys. Rev. Lett.* **102**,

- 218303 (2009); C. Heussinger, P. Chaudhuri, and J.L. Barrat, *Soft Matter* **6**, 3050 (2010).
- [8] M. Mailman, C.F. Schreck, C.S. O'Hern, and B. Chakraborty, *Phys. Rev. Lett.* **102**, 255501 (2009); A. Donev, R. Connelly, F.H. Stillinger, and S. Torquato, *Phys. Rev. E* **75**, 051304 (2007).
- [9] G. Lois, J. Blawdziewicz, and C.S. O'Hern, *Phys. Rev. Lett.* **100**, 028001 (2008).
- [10] Z. Zhang, N. Xu, D.T.N Chen, P. Yunker, A.M. Alsayed, K.P. Aptowicz, P. Habdas, A.J. Liu, S.R. Nagel, and A.G. Yodh, *Nature (London)* **459**, 230 (2009).
- [11] J.A. Drocco, M.B. Hastings, C.J. Olson Reichhardt, and C. Reichhardt, *Phys. Rev. Lett.* **95**, 088001 (2005).
- [12] R. Candelier and O. Dauchot, *Phys. Rev. E* **81**, 011304 (2010).
- [13] S. Bhattacharya and M.J. Higgins, *Phys. Rev. Lett.* **70**, 2617 (1993).
- [14] M.C. Faleski, M.C. Marchetti, and A.A. Middleton, *Phys. Rev. B* **54**, 12427 (1996).
- [15] C.J. Olson, C. Reichhardt, and F. Nori, *Phys. Rev. Lett.* **81**, 3757 (1998).
- [16] C. Reichhardt and C.J. Olson, *Phys. Rev. Lett.* **89**, 078301 (2002).
- [17] A. Pertsinidis and X.S. Ling, *Phys. Rev. Lett.* **100**, 028303 (2008).
- [18] T. Bohlein, J. Mikhael, and C. Bechinger, *Nature Mater.* **11**, 126 (2012).
- [19] G. Grüner, *Rev. Mod. Phys.* **60**, 1129 (1988).
- [20] A.C. Marley, M.J. Higgins, and S. Bhattacharya, *Phys. Rev. Lett.* **74**, 3029 (1995).
- [21] S.S. Banerjee *et al.*, *Phys. Rev. B* **62**, 11838 (2000).
- [22] C.J. Olson Reichhardt and C. Reichhardt, *Phys. Rev. E* **82**, 051306 (2010).
- [23] M. Wyart, L.E. Silbert, S.R. Nagel and T.A. Witten, *Phys. Rev. E* **72**, 051306 (2005).
- [24] D. Vagberg, D. Valdez-Balderas, M.A. Moore, P. Olsson, and S. Teitel, *Phys. Rev. E* **83**, 030303 (2011).
- [25] S. Okuma and N. Kokubo, *Phys. Rev. B* **61**, 671 (2000).